



CENTRE FOR **STOCHASTIC GEOMETRY**
AND ADVANCED **BIOIMAGING**



Ute Hahn and Eva B. Vedel Jensen

Inhomogeneous spatial point processes with hidden second-order stationarity

No. 07, September 2013

Inhomogeneous spatial point processes with hidden second-order stationarity

Ute Hahn and Eva B. Vedel Jensen

Department of Mathematics
Aarhus University
ute@imf.au.dk, eva@imf.au.dk

Abstract

Modelling of inhomogeneous spatial point patterns is a challenging research area with numerous applications in diverse areas of science. In recent years, the focus has mainly been on the class of reweighted second-order stationary point processes that is characterized by the mathematically attractive property of a translation invariant pair correlation function. Motivated by examples where this model class is not adequate, we extend the class of reweighted second-order stationary processes. The extended class consists of hidden second-order stationary point processes for which the pair correlation function $g(u, v)$ is a function of $u \overset{\sim}{-} v$, where $\overset{\sim}{-}$ is a generalized subtraction operator. For the reweighted second-order stationary processes, the subtraction operator is simply $u \overset{\sim}{-} v = u - v$. The processes in the extended class are called hidden second-order stationary because, in many cases, they may be derived from second-order stationary *template* processes. We review and discuss different types of hidden second-order stationarity. Alternatives to reweighted second-order stationarity are retransformed and locally rescaled second-order stationarity. Permutation tests for the different types of hidden second-order stationarity are developed. A test for local anisotropy is also derived. We illustrate our approach by a detailed analysis of three point patterns.

Keywords: Inhomogeneity; Intensity reweighted stationarity; Local scaling; Second-order stationarity; Spatial point processes; Transformation

1 Introduction

Modelling inhomogeneous spatial point patterns with interaction is an active and developing research area of spatial statistics (Møller and Waagepetersen, 2007). Various model classes for such point patterns have been suggested (Baddeley et al., 2000; Hahn et al., 2003; Jensen and Nielsen, 2000), differing in the specification of how the interaction between points depends on the local intensity of points. The most important model classes appear to be the *intensity reweighted*, the *retransformed* and

the *locally rescaled second-order stationary* point processes (Illian et al., 2008, Chapter 4.10). As we shall see, they can all be regarded as hidden second-order stationary. Although statistical inference procedures have been developed for all three model classes, cf. Nielsen and Jensen (2004); Prokešová et al. (2006); Hahn (2007); Møller and Waagepetersen (2007) and references therein, the focus has in recent years been on intensity reweighted second-order stationary point processes, cf. Guan (2008a,b, 2009a,b); Guan and Loh (2007); Guan and Shen (2010); van Lieshout (2011); Møller and Waagepetersen (2007); Waagepetersen (2007); Waagepetersen and Guan (2009).

For ease of exposition, we will exclusively consider spatial point processes in the plane. Any model of how the interaction between points in a point process \mathbf{X} depends on the local intensity of points can be regarded as a kind of mean-variance relationship. Let $\lambda(u)$ be the intensity function of the process. Then, $\lambda(u) du$ is the mean number of points in an infinitesimal region around u with area du . The interaction between points is determined by the second-order product density $\lambda^{(2)}$ of \mathbf{X} . For $u \neq v$, $\lambda^{(2)}(u, v) du dv$ may be interpreted as the probability that there is a point from \mathbf{X} in each of the infinitesimal regions around u and v of area du and dv , respectively. The interaction is described by the 'mean-variance' relationship

$$\lambda^{(2)}(u, v) = g(u, v)\lambda(u)\lambda(v), \quad (1)$$

where $g(u, v)$ is the so-called *pair correlation function* of \mathbf{X} . The model class of reweighted second-order stationary point processes is characterized by translation invariance of the pair correlation function

$$g(u, v) = g(u - v). \quad (2)$$

Processes obtained by independent thinning of stationary processes are reweighted second-order stationary. But there are a number of important point processes that do not satisfy the assumption of reweighted second-order stationarity. One example is processes with hard core distance depending on location. Another example is cluster processes with non-stationary parent process, cf. Hellmund et al. (2008) and Prokešová (2010). However, as we will see later, the pair correlation functions of retransformed and locally rescaled second-order stationary point processes do possess a similar property as (2).

In the present paper, we develop specific procedures for checking the three different types of hidden second-order stationarity mentioned above and illustrate how these procedures work in practice. The permutation test developed in the present paper is a generalization of the recent method published in Hahn (2012), where K -functions estimated on two individual point patterns are compared.

In Section 2, we give a number of examples of point patterns with different types of interaction structure. Section 3 contains a very brief summary of the necessary concepts on spatial point processes needed in the following, while Section 4 discusses the three types of hidden second-order stationarity considered: reweighted, retransformed and locally rescaled second-order stationarity. For each type of hidden second-order stationarity, examples of point process models having this type of interaction structure are given and estimators of the so-called template K -functions are derived. Permutation tests for hidden second-order stationarity are developed in Section 5, and interesting conclusions for the examples are reached in Section 6.

In Section 7, perspectives and future research are discussed. Some derivations are deferred to two appendices.

The proposed estimators and tests have been implemented in an R-package that complements the R-library `spatstat` (Baddeley and Turner, 2006). The programs and data used in the analysis are available for download.

2 Examples of inhomogeneous point patterns

2.1 The bronze data

Figure 1 shows a longitudinal section of a bronze sinter filter that has earlier been analyzed in Hahn et al. (1999) and Hahn (2007). The bronze data show a pronounced direction of inhomogeneity. This is due to the way the specimen was produced: the gradient in the present probe was achieved by successive sedimentation of bronze powders with varying diameter, see Bernhardt et al. (1997). The centers of the particle sections form a non-stationary point pattern. Because of the way the material has been constructed, it is reasonable to assume that the point intensity depends only on one coordinate. Observe also that the interaction structure appears locally scaled in the sense that the local point pattern in dense regions will, after upscaling, appear similar to the local point pattern in sparse regions. This hypothesis of local scaling is justified by the way the material was made.

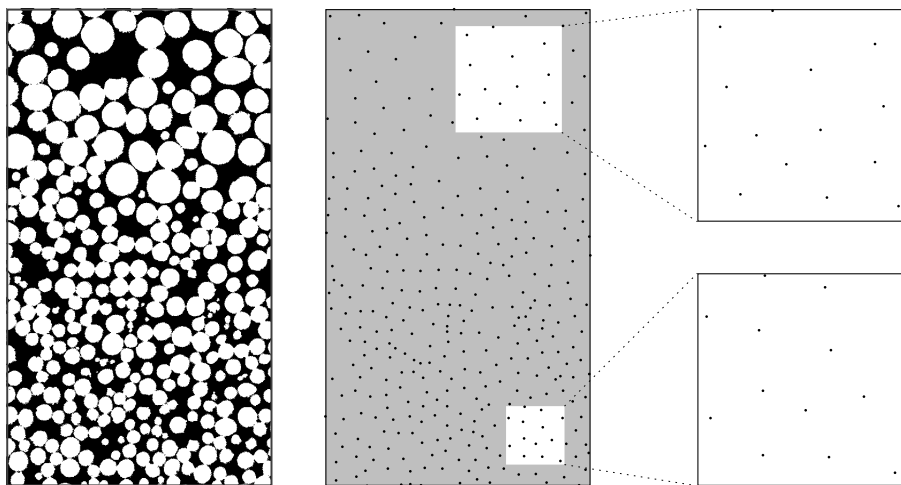


Figure 1: Left part: Portion of a longitudinal section of a bronze sinter filter with a gradient in particle size and number (courtesy B. Kieback and R. Bernhardt, Dresden). Middle part: Centres of particle profiles. Right part: Two enlargements from the top and the bottom of the specimen, containing about the same number of points, show similar geometry. (From Hahn et al. (2003) by permission. Copyright © Applied Probability Trust 2003.)

2.2 The *Beilschmiedia* data

As part of a large-scale study of biodiversity, the positions of 3604 *Beilschmiedia pendula* trees in the tropical rain forest of Barro Colorado Island have been recorded, see Figure 2. The *Beilschmiedia* data comes with additional covariate information

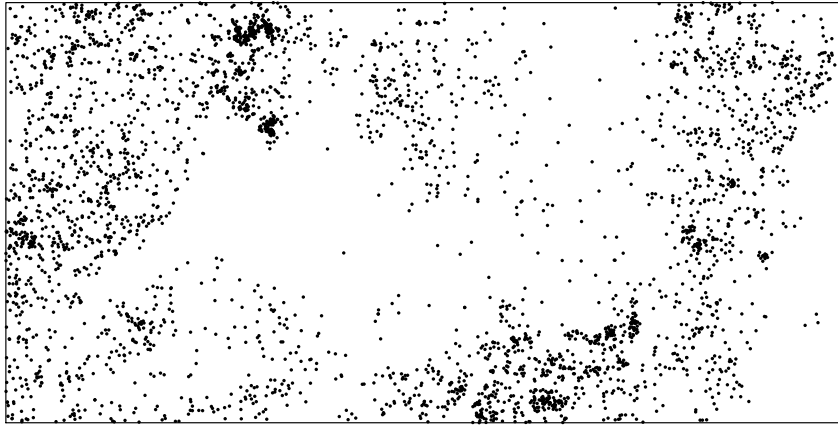


Figure 2: Locations of 3604 *Beilschmiedia pendula* trees in a 1000 m \times 500 m plot in the Central American tropical rain forest.

on the altitude and norm of the altitude gradient. These data have been analyzed in Møller and Waagepetersen (2007), see also Hubbel and Foster (1983), Condit et al. (1996) and Condit (1998). The covariates influence the local intensity of the point pattern. In Møller and Waagepetersen (2007), this dependency is described by a log-linear model for the intensity. The interaction is described by a reweighted second-order stationary Cox process, indicating that there is strong clustering in the point pattern.

2.3 The *Scholtzia* data

Figure 3 depicts a point pattern of 171 individuals of *Scholtzia* aff. *involutrata* in the Australian bush. The pattern has been analyzed in Prokešová et al. (2006), data are from Armstrong (1991). The point intensity is increasing in the North-South direction. For this point pattern, it is less clear how the interaction depends on the local intensity if there is an interaction at all. In Prokešová et al. (2006), a locally scaled area interaction model was used, but since the interaction is not very strong, a model based on location dependent thinning of a stationary process might provide an equally satisfactory description of the data.

3 Spatial point processes

A spatial point process \mathbf{X} on \mathbb{R}^2 is a locally finite random subset of \mathbb{R}^2 . A realization of such a process is a spatial point pattern $\mathbf{x} = \{x_i\}$. In some cases, the process is concentrated on a bounded region of the plane \mathbb{R}^2 .

The process is said to be first-order stationary if its intensity function $\lambda(s)$ is constant. We will mainly be interested in processes that do not possess this property. For instance, the intensity may take a parametric form, depending on an unknown vector β of parameters, such as a log-linear form

$$\lambda(s; \beta) = \exp(\beta \cdot z(s)),$$

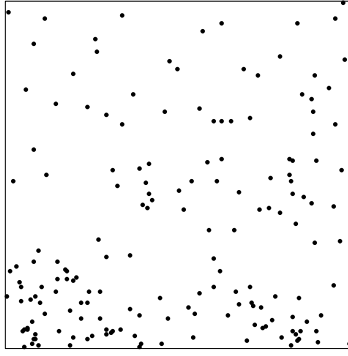


Figure 3: Locations of 171 individuals of *Scholtzia aff. involucrata* in the Australian bush on a $22\text{ m} \times 22\text{ m}$ square. Data from Armstrong (1991), by kind permission.

where $z(s)$ is a vector of covariates evaluated at $s \in \mathbb{R}^2$. This parametric form was used in Waagepetersen (2007) for the *Beilschmiedia* data.

The interaction between points can be described by the pair correlation function

$$g(u, v) = \frac{\lambda^{(2)}(u, v)}{\lambda(u)\lambda(v)}. \quad (3)$$

The process is said to be *second-order stationary* if it is first-order stationary and its pair correlation function is translation invariant, i.e.

$$g(u, v) = g(u - v). \quad (4)$$

For any non-negative measurable function f on $\mathbb{R}^2 \times \mathbb{R}^2$, we have, cf. e.g. Møller and Waagepetersen (2003, p. 31),

$$\mathbb{E} \sum_{u \in \mathbf{X}} \sum_{v \in \mathbf{X} \setminus \{u\}} f(u, v) = \int_{\mathbb{R}^2} \int_{\mathbb{R}^2} f(u, v) \lambda^{(2)}(u, v) du dv. \quad (5)$$

If \mathbf{X} is second-order stationary, it follows for arbitrary subsets $A, B \subseteq \mathbb{R}^2$ that

$$\mathbb{E} \sum_{u \in \mathbf{X}_A} \sum_{v \in \mathbf{X} \setminus \{u\}} \mathbf{1}(u - v \in B) = \lambda^2 |A| \int_B g(u) du, \quad (6)$$

where $\mathbf{1}(\cdot)$ is the indicator function, $|A|$ denotes the area of A and $\mathbf{X}_A = \mathbf{X} \cap A$. In particular, if $|A| > 0$, we have under the assumption of second-order stationarity that

$$\frac{1}{\lambda|A|} \mathbb{E} \sum_{u \in \mathbf{X}_A} \sum_{v \in \mathbf{X} \setminus \{u\}} \mathbf{1}(\|u - v\| \leq r) = \lambda K(r), \quad (7)$$

where

$$K(r) = \int_{B(O, r)} g(u) du \quad (8)$$

is the so-called K -function of \mathbf{X} and $B(O, r)$ is the circular disk with radius r , centred at O . Since the mean number of points from \mathbf{X} in A is $\lambda|A|$, it follows

from (7) that $\lambda K(r)$ can be interpreted as the mean number of further points at a distance at most r from a typical point of \mathbf{X} .

In the following section, we will discuss various ways of introducing inhomogeneity into a number of well-known point process models. A wide class of cluster processes is the Cox processes driven by a non-negative process $\Lambda = \{\Lambda(u)\}$, such that conditional on Λ , \mathbf{X} is a Poisson process with intensity function Λ , cf. Cox (1955), Møller and Waagepetersen (2003), Illian et al. (2008) and references therein. The intensity function and pair correlation function of a Cox process have the following form

$$\lambda(u) = \mathbb{E}\Lambda(u), \quad g(u, v) = \mathbb{E}(\Lambda(u)\Lambda(v))/[\mathbb{E}(\Lambda(u))\mathbb{E}(\Lambda(v))].$$

In particular, we will consider Neyman-Scott processes (Neyman and Scott, 1958) for which

$$\Lambda(u) = \alpha \sum_{c \in \Phi} k(c, u). \quad (9)$$

Here, $\alpha > 0$, Φ is a Poisson point process with intensity function ρ , say, and $k(c, \cdot)$ is a probability density for a two-dimensional continuous random variable. These processes are Poisson cluster processes that can be constructed as $\mathbf{X} = \cup_{c \in \Phi} \mathbf{X}_c$ where $\{\mathbf{X}_c\}$ are independent and identically distributed, the number of points in \mathbf{X}_c is Poisson distributed with parameter α and the points in \mathbf{X}_c are independent and identically distributed with density $k(c, \cdot)$. The special case of the Thomas process (Thomas, 1949) is obtained by letting $k(c, u) = \phi(u-c; \sigma)$ where $\phi(\cdot; \sigma)$ is the density of the two-dimensional normal distribution with mean 0 and covariance matrix $\sigma^2 I$. Another important subclass is the Matérn cluster processes (Matérn, 1960) for which $k(c, u) = \mathbf{1}(\|u - c\| \leq r)/[\pi r^2]$. Usually the Thomas and Matérn cluster processes are considered in the case where the Poisson process Φ is first-order stationary with intensity κ , say, but we will here also study the case of non-stationary Φ . The intensity function and pair correlation function of the Neyman-Scott process with random intensity given in (9) take the form

$$\lambda(u) = \alpha \int_{\mathbb{R}^2} \rho(x) k(x, u) dx,$$

$$g(u, v) = \frac{\int_{\mathbb{R}^2} \rho(x) k(x, u) k(x, v) dx}{\int_{\mathbb{R}^2} \rho(x) k(x, u) dx \int_{\mathbb{R}^2} \rho(x) k(x, v) dx} + 1.$$

We will also in the following section give examples of how to introduce inhomogeneity into point process models with repulsion between points. One of the models to be considered is the Matérn hard core process. Such a process can be obtained by thinning of a homogeneous Poisson process Φ with intensity κ in the following manner

$$\mathbf{X} = \{x \in \Phi \mid U_x < U_y \text{ for all } y \in \Phi \text{ with } 0 < \|y - x\| \leq r\},$$

where $\{U_x \mid x \in \Phi\}$ is a sequence of independent and identically uniformly distributed random variables on $[0, 1]$, independent of Φ , and r is the hard core distance. If we parameterize the process by r and the scale invariant parameter $\eta = \kappa \pi r^2$ and let

$$\Gamma_r(u) = |B(O, r) \cup B(u, r)| = \pi r^2 \gamma_1\left(\frac{u}{r}\right),$$

say, then the intensity function and the pair correlation function of the Matérn hard core process are

$$\lambda(u) = \frac{1 - \exp(-\eta)}{\pi r^2}, \quad g(u, v) = g_1\left(\frac{u - v}{r}\right),$$

where

$$g_1(u) = \mathbf{1}(\|u\| > 1) 2 \frac{\gamma_1(u)(1 - \exp(-\eta)) - (1 - \exp(-\eta\gamma_1(u)))}{\gamma_1(u)(\gamma_1(u) - 1)(1 - \exp(-\eta))^2}.$$

4 Hidden second-order stationarity

Below, we will define and discuss different models for hidden second-order stationarity of inhomogeneous spatial point processes \mathbf{X} and provide examples of inhomogeneous point process models that possess the types of hidden second-order stationarity under consideration. In all cases considered, the pair correlation function is of the form

$$g(u, v) = g_0(u \overset{\smile}{-} v), \quad (10)$$

where $\overset{\smile}{-} : \mathbb{R}^2 \times \mathbb{R}^2 \rightarrow \mathbb{R}^2$ is a generalized subtraction operator, satisfying

$$u \overset{\smile}{-} v = -(v \overset{\smile}{-} u). \quad (11)$$

In the case of reweighted and retransformed second-order stationarity, $\overset{\smile}{-}$ also fulfils

$$u \overset{\smile}{-} v + v \overset{\smile}{-} w = u \overset{\smile}{-} w. \quad (12)$$

In the case of locally rescaled second-order stationarity, (12) holds locally.

In a number of cases, the process \mathbf{X} may be derived from a second-order stationary *template* process \mathbf{X}_0 with pair correlation function g_0 . For this reason, we will generally denote the function g_0 in (10) the *template g-function* and

$$K_0(r) = \int_{B(O, r)} g_0(r) \, du$$

the *template K-function*.

4.1 Reweighted second-order stationarity

A point process \mathbf{X} with intensity function λ is said to be reweighted second-order stationary, if the second-order product density of \mathbf{X} is of the following form (Baddeley et al., 2000)

$$\lambda^{(2)}(u, v) = g_0(u - v)\lambda(u)\lambda(v), \quad (13)$$

or, equivalently, \mathbf{X} has pair correlation function $g(u, v) = g_0(u - v)$. Here, the subtraction operator $\overset{\smile}{-}$ is simply

$$u \overset{\smile}{-} v := u - v. \quad (14)$$

One way of constructing a reweighted second-order stationary point process \mathbf{X} with intensity function λ , bounded from above by λ_{\max} , is to apply location dependent thinning to a second-order stationary process \mathbf{X}_0 with intensity λ_{\max} and pair

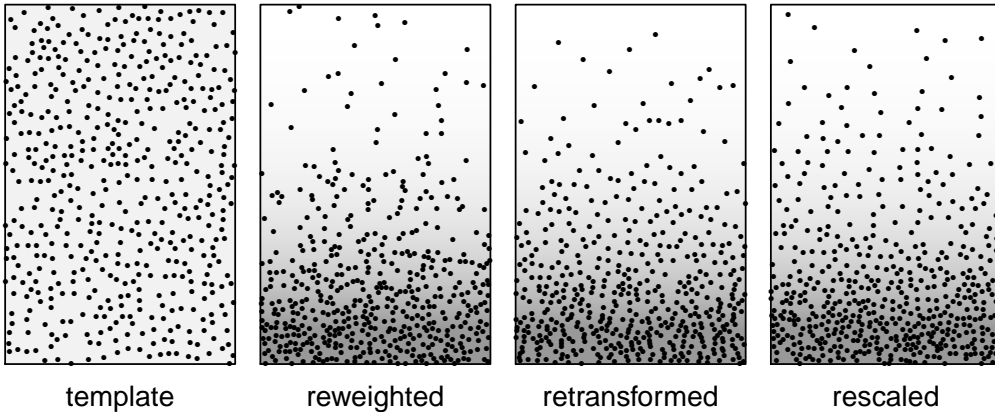


Figure 4: Realizations of reweighted, retransformed and locally rescaled second-order stationary point processes, sharing (up to a scale factor) the same template process, which is a homogeneous Matérn hard core process \mathbf{X}_0 with shape parameter $\eta = 10$. The three inhomogeneous processes have all the same intensity function, depicted as a gray value image.

correlation function $g_0(u, v) = g_0(u - v)$ identical to the pair correlation function of \mathbf{X} . The reweighted second-order stationary process is obtained as

$$\mathbf{X} = \left\{ v \in \mathbf{X}_0 \mid U_v \leq \frac{\lambda(v)}{\lambda_{\max}} \right\},$$

where $\{U_v \mid v \in \mathbf{X}_0\}$ is a sequence of independent and identically uniformly distributed random variables on $[0, 1]$, independent of \mathbf{X}_0 . If \mathbf{X}_0 is Poisson, then the thinned process \mathbf{X} is also Poisson. Note that a reweighted second-order stationary process with unbounded intensity function cannot be obtained by such a thinning.

Figure 4 shows a realization of a reweighted second-order stationary process (second from the left), obtained by thinning of a homogeneous Matérn hard core process. A realization of this template is, up to a scale factor, shown to the left in Figure 4. Note the Poisson-like appearance of the sparse part of the reweighted second-order stationary process.

A wide class of point processes satisfying (13) is Cox processes with random intensity function Λ given by

$$\log \Lambda(u) = x(u) + \Psi(u),$$

where $x = \{x(u)\}$ is a deterministic function and $\Psi = \{\Psi(u)\}$ is a strictly stationary process.

Examples of point processes that do not satisfy the assumption of reweighted second-order stationarity are processes with location dependent hard core distance and cluster processes with non-stationary parent process, see also Prokešová (2010). Let us first consider the processes with location dependent hard core. Let us assume that there exists a positive, non-constant function $r(u)$ satisfying $\lambda^{(2)}(u, v) = 0$ for all $v \in B(u, r(u)) \setminus \{u\}$ and $r(u)$ is maximal having this property. Since $r(u)$ is non-constant, we can find u_1, u_2 such that $r(u_1) < r(u_2)$. Then, there exists $v \in B(u_1, r(u_2)) \setminus \{u_1\}$ with $\lambda^{(2)}(u_1, v) > 0$ but

$$\lambda^{(2)}(u_2, v + u_2 - u_1) = 0$$

since $v + u_2 - u_1 \in B(u_2, r(u_2)) \setminus \{u_2\}$. Then, $g(u, v)$ is not translation invariant.

Cluster processes with non-stationary parent process have been considered for modelling species in forest communities. For instance, in Shimatani and Kubota (2004), a Thomas process with an inhomogeneous Poisson point process with intensity ρ as parent process is used. The pair correlation function takes the following form in this case

$$g(u, v) = \frac{\int_{\mathbb{R}^2} \rho(x) \varphi(u - x; \sigma) \varphi(v - x; \sigma) dx}{\int_{\mathbb{R}^2} \rho(x) \varphi(u - x; \sigma) dx \int_{\mathbb{R}^2} \rho(x) \varphi(v - x; \sigma) dx} + 1. \quad (15)$$

The pair correlation function given in (15) is obviously not always translation invariant, but will be in the special case where ρ is constant.

It can be shown, using (5), that (13) implies that the template K -function satisfies

$$K_0(r) = \frac{1}{|A|} \mathbb{E} \sum_{u \in \mathbf{X}_A} \sum_{v \in \mathbf{X} \setminus \{u\}} \frac{\mathbf{1}(\|u - v\| \leq r)}{\lambda(u)\lambda(v)}. \quad (16)$$

An unbiased estimate of the template K -function is therefore under reweighted second-order stationarity simply

$$\hat{K}_0^{(w)}(r) = \frac{1}{|A|} \sum_{u \in \mathbf{X}_A} \sum_{v \in \mathbf{X} \setminus \{u\}} \frac{\mathbf{1}(\|u - v\| \leq r)}{\lambda(u)\lambda(v)}.$$

If observation is available only inside A , then the following edge-corrected unbiased estimate may be used

$$\hat{K}_0^{(w)}(r) = \sum_{u \in \mathbf{X}_A} \sum_{v \in \mathbf{X}_A \setminus \{u\}} \frac{\mathbf{1}(\|u - v\| \leq r)}{\lambda(u)\lambda(v)|A \cap A_{u-v}|}. \quad (17)$$

This estimator can be written in the form

$$\hat{K}_0^{(w)}(r) = \frac{1}{|A|} \sum_{u \in \mathbf{X}_A} \sum_{v \in \mathbf{X}_A \setminus \{u\}} \frac{\mathbf{1}(\|u - v\| \leq r) w_A(u, v)}{\lambda(u)\lambda(v)}, \quad (18)$$

with translational edge correction

$$w_A(u, v) = \frac{|A|}{|A \cap A_{u-v}|},$$

cf. Møller and Waagepetersen (2007, Section 6.2). An alternative for the case of isotropic pair correlation, as given in Baddeley et al. (2000), uses Ripley's (1976) isotropic edge correction factor

$$w_A(u, v) = \frac{L(\partial B(u, \|u - v\|))}{L(\partial B(u, \|u - v\|) \cap A)} = \frac{2\pi\|u - v\|}{L(\partial B(u, \|u - v\|) \cap A)}, \quad (19)$$

where $L(\partial B(u, \|u - v\|) \cap A)$ is the length inside A of the boundary of the ball around u through v .

4.2 Retransformed second-order stationarity

Let \mathbf{X}_0 be a second-order stationary process with intensity λ_0 . Let $h : \mathbb{R}^2 \rightarrow \mathbb{R}^2$ be a one-to-one differentiable transformation and let Jh^{-1} be the Jacobian of the inverse transformation. Then, $\mathbf{X} = h(\mathbf{X}_0)$ has intensity function $\lambda(\cdot) = \lambda_0 Jh^{-1}(\cdot)$ and, using (5), it follows that \mathbf{X} has pair correlation function

$$g(u, v) = g_0(h^{-1}(u) - h^{-1}(v)), \quad (20)$$

where $g_0(u, v) = g_0(u - v)$ is the pair correlation function of \mathbf{X}_0 .

Motivated by this, a point process \mathbf{X} with intensity function λ is said to be retransformed second-order stationary if we can find a one-to-one differentiable (up to a set of Lebesgue measure zero) transformation $h : \mathbb{R}^2 \rightarrow \mathbb{R}^2$, such that

$$\lambda(u) = \lambda_0 Jh^{-1}(u) \quad (21)$$

for some $\lambda_0 > 0$ and

$$\lambda^{(2)}(u, v) = g_0(h^{-1}(u) - h^{-1}(v)) \lambda(u) \lambda(v) \quad (22)$$

for some function g_0 on \mathbb{R}^2 . Then, λ_0 and g_0 are the intensity and pair correlation function of the second-order stationary process $\mathbf{X}_0 = h^{-1}(\mathbf{X})$. For retransformed second-order stationary point processes, the generalized subtraction operator is given by

$$u \dot{-} v = h^{-1}(u) - h^{-1}(v). \quad (23)$$

If the template process \mathbf{X}_0 is Poisson, then the transformed process $\mathbf{X} = h(\mathbf{X}_0)$ is also Poisson.

Figure 4 shows a realization of a retransformed second-order stationary process (second from the right), obtained by transformation of a homogeneous Matérn hard core process. Note the local anisotropy, especially in the dense part of the process where the nearest neighbour tends to be located in the vertical direction.

Retransformed second-order stationary point processes constitute a natural model class primarily in the case where the observed point pattern is the result of a physical transformation (stretching/squeezing) of a second-order stationary point process. In Appendix A, transformations are constructed for the case where λ depends on one coordinate only or on the distance to a reference point.

A wide class of point processes satisfying (22) is Cox processes with random intensity function given by

$$\Lambda(u) = Jh^{-1}(u) \Lambda_0(h^{-1}(u)),$$

where h is a one-to-one differentiable transformation and $\Lambda_0 = \{\Lambda_0(u)\}$ is a strictly stationary process.

Transformation of Markov point processes has been considered in Jensen and Nielsen (2000, 2001). As an example, let \mathbf{X}_0 be a pairwise interaction process with density with respect to the unit rate Poisson process of the form

$$f_{\mathbf{X}_0}(x) \propto \beta^{n(x)} \prod_{u, v \in x}^{\neq} \gamma(\|u - v\|). \quad (24)$$

Then, it can be shown that the density of $\mathbf{X} = h(\mathbf{X}_0)$ with respect to the unit rate Poisson process is given by

$$f_{\mathbf{X}}(x) \propto \beta^{n(x)} \prod_{u \in x} Jh^{-1}(u) \prod_{\substack{\neq \\ u, v \in x}} \gamma(\|h^{-1}(u) - h^{-1}(v)\|). \quad (25)$$

Note that if $\gamma(d) = 1$ for $d > r$, then \mathbf{X}_0 is Markov with respect to the relation

$$u \sim v \quad \Leftrightarrow \quad \|u - v\| < r.$$

In this case, the transformed process will be Markov with respect to an induced relation

$$u \approx v \quad \Leftrightarrow \quad \|h^{-1}(u) - h^{-1}(v)\| < r.$$

For further details, see Jensen and Nielsen (2000). Note also that the template process \mathbf{X}_0 with density specified in (24) is not strictly second-order stationary because the process is defined on a bounded subset of \mathbb{R}^2 .

For a retransformed second-order stationary process, $\mathbf{X}_0 = h^{-1}(\mathbf{X})$ is second-order stationary with λ_0 and g_0 as intensity and pair correlation function. It follows that the template K -function $K_0(r) = \int_{B(O,r)} g_0(u) du$ of a retransformed second-order stationary process \mathbf{X} satisfies

$$K_0(r) = \frac{1}{|h^{-1}(A)|} \frac{1}{\lambda_0^2} \mathbb{E} \sum_{u \in \mathbf{X}_A} \sum_{v \in \mathbf{X} \setminus \{u\}} \mathbf{1}(\|h^{-1}(u) - h^{-1}(v)\| \leq r),$$

An unbiased estimate of the template K -function is therefore

$$\widehat{K}_0^{(t)}(r) = \frac{1}{|h^{-1}(A)|} \frac{1}{\lambda_0^2} \sum_{u \in \mathbf{X}_A} \sum_{v \in \mathbf{X} \setminus \{u\}} \mathbf{1}(\|h^{-1}(u) - h^{-1}(v)\| \leq r).$$

If observation is available only inside A , then the following edge-corrected estimate of the template K -function may be used

$$\widehat{K}_0^{(t)}(r) = \frac{1}{\lambda_0^2} \sum_{u \in \mathbf{X}_A} \sum_{v \in \mathbf{X}_A \setminus \{u\}} \frac{\mathbf{1}(\|h^{-1}(u) - h^{-1}(v)\| \leq r)}{|h^{-1}(A) \cap h^{-1}(A)_{(h^{-1}(u) - h^{-1}(v))}|}. \quad (26)$$

4.3 Locally rescaled second-order stationarity

Let \mathbf{X}_0 be an isotropic second-order stationary process with intensity 1 and pair correlation function g_0 . Let $c > 0$. Then, the scaled process $\mathbf{X} = c\mathbf{X}_0$ has intensity $\lambda = c^{-2}$ and second-order product density of the form

$$\lambda^{(2)}(u, v) = g_0(\sqrt{\lambda}\|u - v\|) \lambda^2. \quad (27)$$

In this subsection, we will study point processes that locally have the property (27). These processes are called locally rescaled second-order stationary. As we shall see, it is generally only possible to derive approximate results for the locally rescaled second-order stationary point processes. This is in contrast to what is obtainable for reweighted and retransformed second-order stationary processes.

A point process \mathbf{X} with intensity function λ is said to be locally rescaled second-order stationary if its second-order product density is of the form

$$\lambda^{(2)}(u, v) = g_0\left(\frac{d_\lambda(u, v)}{\|u - v\|}(u - v)\right)\lambda(u)\lambda(v), \quad (28)$$

where d_λ is the locally scaled distance

$$d_\lambda(u, v) = \int_{[u, v]} \sqrt{\lambda(w)} \, dw.$$

Note that if λ is constant on $[u, v]$, then d_λ is proportional to Euclidean distance and (28) reduces to (27). In case $g_0(u - v) = g_0(\|u - v\|)$, (28) simplifies to

$$\lambda^{(2)}(u, v) = g_0(d_\lambda(u, v))\lambda(u)\lambda(v). \quad (29)$$

Note that if \mathbf{X} is a second-order stationary point process with intensity λ and pair correlation $g(u - v)$, then \mathbf{X} is locally rescaled second-order stationary with template pair correlation function $g_0(u) = g(u/\sqrt{\lambda})$.

The subtraction operator is given by

$$u \overset{\sim}{-} v := (u - v)d_\lambda(u, v)/\|u - v\|. \quad (30)$$

The operator (30) clearly fulfils $u \overset{\sim}{-} v = -(v \overset{\sim}{-} u)$, but the transitive property (12) will in general only hold approximately and locally for u, v, w so close that λ is approximately constant on the triangle spanned by u, v, w . If indeed λ is constant on the triangle, (12) holds exactly for this choice of triplet.

Let us construct a locally scaled version of a stationary and isotropic Neyman-Scott process \mathbf{X}_0 . For \mathbf{X}_0 , we have a Poisson distributed number of offsprings with parameter α around each parent and the offsprings are distributed according to the probability density $k(\|\cdot - u\|)$ around a parent at position u . The intensity of parents in \mathbf{X}_0 is taken to be α^{-1} such that the intensity of \mathbf{X}_0 becomes $\alpha^{-1}\alpha = 1$. Let $c(x) > 0$, $x \in \mathbb{R}^2$, be a scaling function. This function is used to change the intensity function of the parents as well as the distribution of the offsprings around the parents. The resulting process Φ of parents is Poisson with intensity function $\alpha^{-1}c(x)^{-2}$. If $u \in \Phi$, the number of offsprings around u is Poisson distributed with parameter α and, conditional on this number, the offsprings around u are independent and identically distributed with density

$$c(u)^{-2}k(c(u)^{-1}\|v - u\|), \quad v \in \mathbb{R}^2.$$

Let us assume that the scaling function is slowly varying compared to the interaction range. For instance, suppose that there exists $r > 0$ such that $k(\|u\|) = 0$ for $\|u\| > r$ and the scaling function satisfies

$$c(v) \approx c(u) \quad \text{for all } u \in \mathbb{R}^2, v \in B(u, c(u)r).$$

Then, the locally scaled Neyman-Scott process \mathbf{X} approximately satisfies (29), as shown in Appendix B.

A locally scaled version of a Matérn hard core process can be constructed as follows. Let $c(x) > 0$, $x \in \mathbb{R}^2$, be a scaling function and let Φ be a Poisson process with intensity function $\alpha^{-1}c(x)^{-2}$. The locally scaled Matérn hard core process is now defined by

$$\mathbf{X} = \{x \in \Phi \mid U_x < U_y \text{ for all } y \in \Phi \text{ with } 0 < d_{c^{-2}}(x, y) = \int_{[x, y]} c(w)^{-1} dw \leq r\}.$$

In Hahn (2007, p. 55 – 56), the intensity and pair correlation functions of \mathbf{X} are derived. Under the assumption of a slowly varying scaling function, (29) is approximately fulfilled. A realization of a locally scaled Matérn hard core process is show in Figure 4 (right). Note that this process has a locally isotropic appearance.

Local scaling of the pairwise interaction process \mathbf{X}_0 with density (24) is considered in Hahn et al. (2003). The locally scaled process \mathbf{X} is obtained by considering the specified density (24) of the template \mathbf{X}_0 as a density with respect to an inhomogeneous Poisson process with intensity λ and substitute the Euclidean distances with scaled distances d_λ . The resulting density of \mathbf{X} with respect to the unit rate Poisson process becomes

$$f_{\mathbf{X}}(x) \propto \beta^{n(x)} \prod_{u \in x} \lambda(u) \prod_{\substack{u, v \in x \\ u \neq v}} \gamma(d_\lambda(u, v)).$$

We can develop estimates of the template K -function $K_0(r) = \int_{B(O, r)} g_0(u) du$ evaluated at r if λ is 'slowly varying' in the locally scaled balls

$$B_\lambda(u, r) = \{v \in \mathbb{R}^2 : d_\lambda(u, v) \leq r\}$$

centred at u with radius r . We focus on the case where $g_0(u - v) = g_0(\|u - v\|)$. We thus require that $B_\lambda(u, r) \approx B(u, r/\sqrt{\lambda(u)})$ and

$$\lambda(v) \approx \lambda(u), \quad \text{for all } v \in B_\lambda(u, r).$$

Then, the template K -function at r is approximately

$$K_0(r) \approx \frac{1}{\mu(A)} \mathbb{E} \sum_{u \in \mathbf{X}_A} \sum_{v \in \mathbf{X} \setminus \{u\}} \mathbf{1}(d_\lambda(u, v) \leq r),$$

where $\mu(A)$ is the mean number of points from \mathbf{X} in A . An approximately unbiased estimate of the template K -function takes the form

$$\widehat{K}_0^{(s)}(r) = \frac{1}{\mu(A)} \sum_{u \in \mathbf{X}_A} \sum_{v \in \mathbf{X} \setminus \{u\}} \mathbf{1}(d_\lambda(u, v) \leq r).$$

If observation is available only inside A , we suggest to use the following estimate of the template K -function

$$\widehat{K}_0^{(s)}(r) = \frac{1}{\mu(A)} \sum_{u \in \mathbf{X}_A} \sum_{v \in \mathbf{X}_A \setminus \{u\}} \mathbf{1}(d_\lambda(u, v) \leq r) w_A(u, v), \quad (31)$$

where w_A is Ripley's edge correction as given in Equation (19), cf. Hahn (2007, Section 4.2.2).

5 Testing hidden second-order stationarity

5.1 Tests based on the K -function

In this section, we present a general method to test the hypothesis that a given point pattern can be ascribed to a reweighted, retransformed or locally rescaled second-order stationary point process model. The tests are based on estimates of the corresponding template K -functions. Under the hidden second-order stationarity in question, the mean of the estimators (18), (26) or (31) of the appropriate template K -function does not depend on the choice of the observation window, in particular not on the local intensity. However under an alternative type of hidden second-order stationarity, the means of the — now inappropriate — estimators do differ, as shown in Figures 5 and 6 for inhomogeneous versions of Matérn hard core and cluster point processes. Only retransformed and locally rescaled point processes seem to be vice versa indistinguishable in that way. The idea of the test is to compare estimates of the template K -function obtained in regions of different intensity. Similarly, Illian et al. (2008, p. 282) suggest to compare reweighted pair correlation functions estimated in subwindows with constant intensity, without giving a formal test. Explorative methods of comparing local K -functions (or L -functions) have earlier been described without the development of a formal test (Getis and Franklin, 1987; Anselin, 1989, 1995; Cressie and Collins, 2001b,a), under the heading of local indicators of spatial association (LISA).

The test described below is a generalization of the method presented in Hahn (2012) for comparison of the K -functions estimated on two individual point patterns.

Let A denote the observation window.

1. Determine $m = m_1 + m_2$ disjoint quadrats $A_1, \dots, A_m \subset A$. The indices are chosen with increasing mean intensity, i.e. $\bar{\lambda}_1 \leq \bar{\lambda}_2 \leq \dots \leq \bar{\lambda}_m$, where $\bar{\lambda}_i = \mu(A_i)/|A_i|$. Let $I_1 = \{1, \dots, m_1\}$ and $I_2 = \{m_1 + 1, \dots, m_1 + m_2\}$ denote the index sets of the quadrats with low and high intensity.
2. On the quadrats, obtain estimates $\hat{K}_1(r), \dots, \hat{K}_m(r)$ of the template K -function under the null hypothesis, using an unbiased estimator.
3. Let

$$\bar{K}_i(r) = \frac{1}{m_i} \sum_{j \in I_i} \hat{K}_j(r), \quad i = 1, 2$$

and

$$s_i^2(r) = \frac{1}{m_i - 1} \sum_{j \in I_i} (\hat{K}_j(r) - \bar{K}_i(r))^2$$

denote mean and empirical variance of the K -function estimates on the two subsets. Since the estimators used are unbiased, $\mathbb{E}\bar{K}_1 = \mathbb{E}\bar{K}_2$ under the null hypothesis.

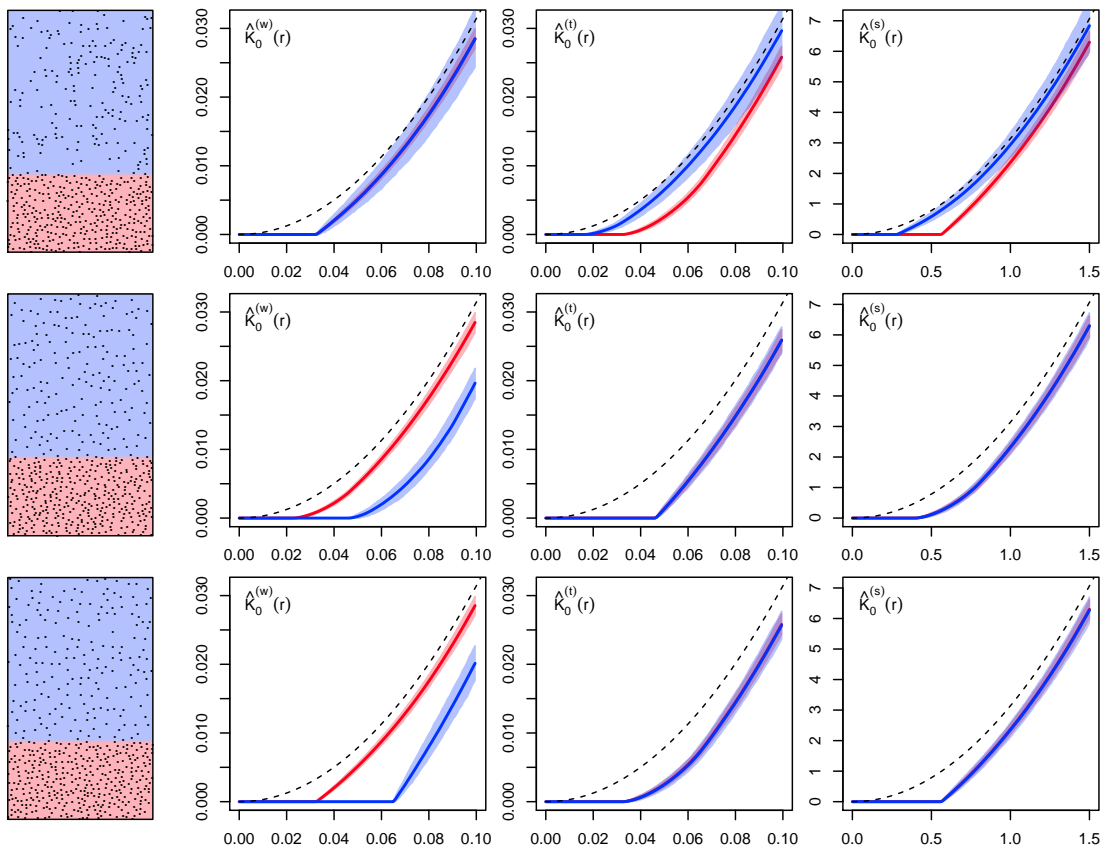


Figure 5: Left: Realizations of reweighted, retransformed and locally rescaled second-order stationary Matérn hard core point processes (top to bottom) with the same template and same intensity function. Right: means and 90% pointwise envelopes of the estimated reweighted, retransformed and locally rescaled K -functions (left to right), estimated from 500 realizations on the subwindows of high and low intensity (red and blue), together with the Poisson K -function (dashed). Mean number of points per pattern: 555.

4. Calculate the test statistic

$$T(I_1, I_2) := \int_0^{r_0} \frac{(\bar{K}_1(r) - \bar{K}_2(r))^2}{(s_1^2(r)/m_1 + s_2^2(r)/m_2)} dr. \quad (32)$$

5. The significance of the studentized distance T between \bar{K}_1 and \bar{K}_2 is assessed by a permutation test. This idea originates from Diggle et al. (1991, 2000), but the test statistic suggested there may lead to size distortion of the test, in particular when the variance of the K -estimates for the two subsets is very different, see Hahn (2012).

The p -value is then obtained by ranking $T(I_1, I_2)$ among all possible outcomes $T(I_1^*, I_2^*)$, with I_1^* running through all subsets of I with cardinality m_1 , and $I_2^* = I \setminus I_1^*$.

Thus, $\binom{m_1+m_2}{m_1}$ partitions of I have to be considered if $m_1 \neq m_2$; for symmetry reasons, only $\binom{m_1+m_2}{m_1}/2$ partitions have to be generated if $m_1 = m_2$.

For larger samples, with $m > 20$, an exact permutation test would create an enormous computational load and should therefore be replaced by a bootstrap test. To

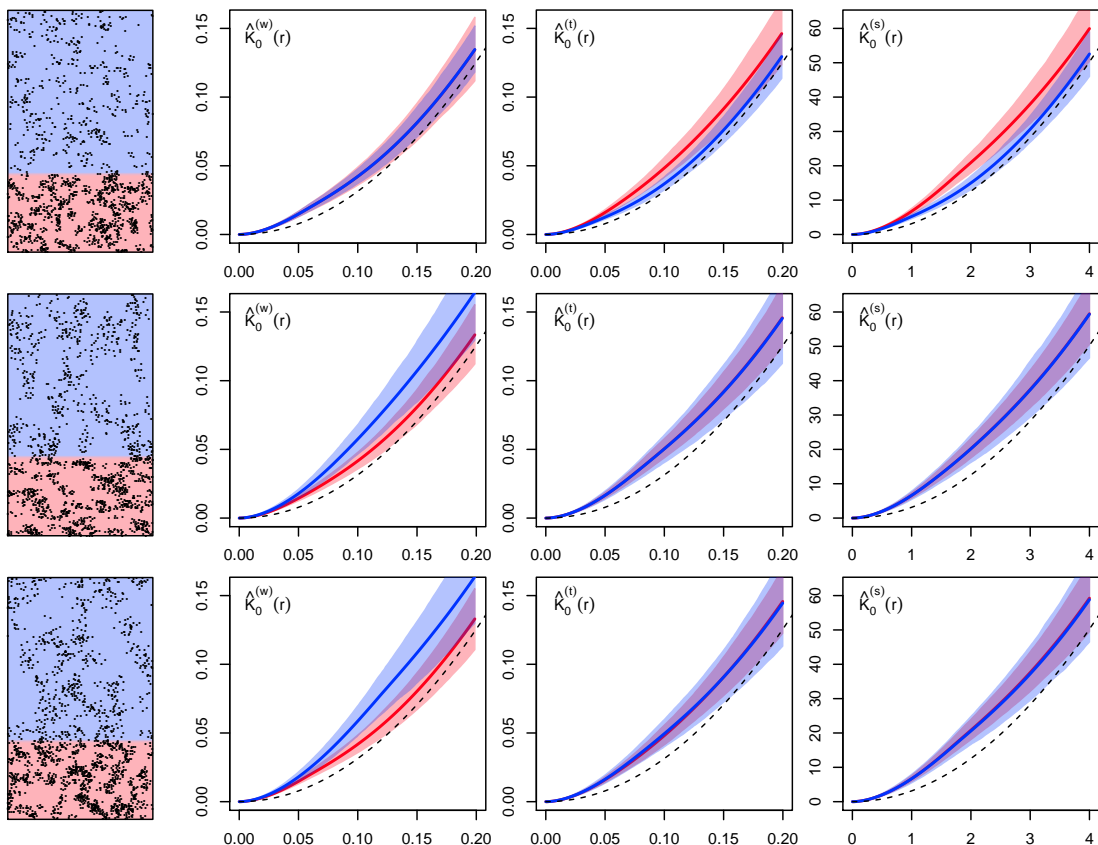


Figure 6: Hidden second-order stationary Matérn cluster point processes and estimates of template K -functions, as in Figure 5; mean number of points per pattern: 1665.

this end, a predefined number n_{boot} of subsets I_1^* and $I_2^* = I \setminus I_1^*$ is randomly generated. The bootstrap p -value is then obtained from the rank of the observed test statistic among the simulated outcomes $T(I_1^*, I_2^*)$.

To achieve the best performance of the test in terms of size and power, the estimators \hat{K}_i should have approximately the same variance. The variance depends largely on the number of points; therefore, the quadrats A_1, \dots, A_m should contain roughly the same number of points. If this is not feasible, we recommend to use the test statistic

$$\bar{T}(I_1, I_2) := \frac{\int_0^{r_0} \frac{1}{r^2} (\bar{K}_1(r) - \bar{K}_2(r))^2 dr}{\int_0^{r_0} \frac{1}{r^2} (s_1^2(r)/m_1 + s_2^2(r)/m_2) dr} \quad (33)$$

instead of T to increase the robustness against heteroskedasticity (Hahn, 2012), at the cost of a loss in power when testing regular point patterns.

An important parameter that influences the power of the tests is the upper integration bound r_0 . It should ideally be chosen such that the most significant differences between the subpatterns under the alternative are covered. For model tests based on similar statistics, it is usually recommended to set $r_0 = 1.25/\sqrt{\lambda}$. This choice goes back to Ripley (1979) and has been thoroughly investigated by Ho and Chiu (2006). In an exemplary simulation study with inhomogeneous regular and clustered point patterns (not shown here), we found $r_0 = 1.25/\sqrt{\lambda_0}$ with $\lambda_0 = \max_{x \in A} \lambda(x)$ to yield more powerful tests in connection with the reweighted K -

function than $r_0 = 2.5/\lambda_0$. For tests based on the rescaled K -function, this is to be replaced by $r_0 = 1.25$, since the template then has unit intensity.

5.2 Directional diagnostics

It is virtually impossible to distinguish between retransformed and locally rescaled second-order stationary models with the above described test, see Figures 5 and 6. Still, these two approaches to generate inhomogeneity lead to different point processes if applied to the same stationary template process: while the locally rescaled version is locally isotropic, the retransformed second-order stationary point pattern exhibits local anisotropy. The K -function is intrinsically isotropic, and therefore not capable to capture this difference.

Transformation generally results in local anisotropy, except if the point process is Poisson. This fact is traditionally exploited in geology to determine the strain rocks with distinguishable particles have been exposed to. Fry (1979) suggests to consider the direction of all segments connecting pairs of particle centres; however, he assumes stationarity. Similarly, Stoyan and Beneš (1991) propose to use the so-called point-pair rose density to describe anisotropy in a stationary point process.

In the present case of retransformed second-order stationary point processes, one may study the nearest neighbour orientation: if the transformation is contractive and an isotropic point pattern \mathbf{X}_0 is locally “squeezed” along one direction, nearest neighbours will preferably occur in that direction. Local “stretching”, on the other hand, leads to a preference of nearest neighbour orientation perpendicular to the transformation direction. However, this only holds for regular point patterns, as already pointed out by Fry (1979). As shown in Figure 7, the effect of strain on clustered patterns is quite different: If the clusters themselves consist of independent points, the process behaves locally almost like a Poisson point process. The – very vague – difference in the rose of nearest neighbour orientations for the two subpatterns is due to a change in the shape of the clusters. In the case of cluster point processes, nearest neighbour orientations are not suitable as a basis for a test, however, in case of regular point patterns, they provide a valuable tool for explorative data analysis and visualization.

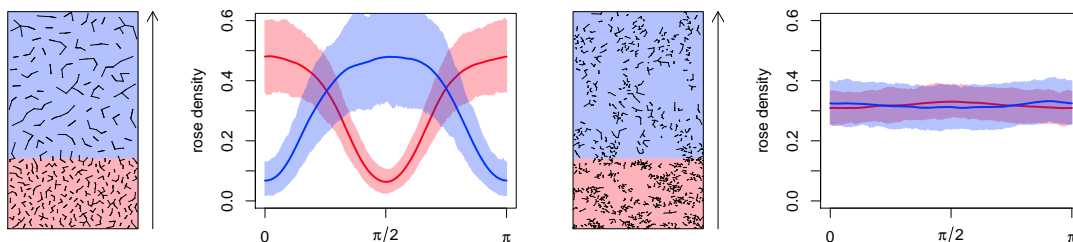


Figure 7: Realizations of retransformed second-order stationary point processes (cf. Figs. 5 and 6), and corresponding rose densities of nearest neighbour orientations. The patterns are shown with segments connecting nearest neighbour pairs; arrow: reference zero direction. Plots of nearest neighbour orientation rose density on the subwindows of high and low intensity (red and blue) show means and 90% pointwise envelopes based on edge corrected kernel estimates from 500 simulated realizations.

A better test statistic is the directional K -function, defined as the integral of the pair correlation function over a sector, cf. Ohser and Stoyan (1981). Since the sign of direction does not matter in orientational analysis, we consider double sectors instead, and define the orientational template K -function with respect to the reference direction vector η as

$$K_0(r; \eta, \delta) := \int_{S(O, r, \eta, \delta)} g_0(u) du, \quad 0 < \delta \leq \pi/2, \quad (34)$$

with

$$S(O, r, \eta, \delta) = \{u \in \mathbb{R}^2 : \|u\| \leq r, |\langle \eta, u \rangle| > \|u\| \cos \delta\},$$

where $\langle \eta, u \rangle$ denotes the scalar product of η and u , $|\eta| = 1$. The angle δ gives half the sector width, thus $K_0(r; \eta, \pi/2) = K_0(r)$.

Under the hypothesis of local rescaling, the orientational template K -function may be estimated analogously to (31), however, the edge correction has to be adapted:

$$\widehat{K}_0^{(s)}(r; \eta, \delta) = \frac{1}{\mu(A)} \sum_{u \in \mathbf{X}_A} \sum_{v \in \mathbf{X}_A \setminus \{u\}} \mathbf{1}(d_\lambda(u, v) \leq r) \cdot \mathbf{1}(|\langle \eta, (v - u) \rangle| > \|v - u\| \cos \delta) w_A(u, v, \eta, \delta), \quad (35)$$

where

$$w_A(u, v, \eta, \delta) = \frac{L(C(u, \|v - u\|))}{L(C(u, \|v - u\|) \cap A)} = \frac{4\delta \|v - u\|}{L(C(u, \|v - u\|) \cap A)}$$

and for $d > 0$

$$C(u, d) = \{w \in \mathbb{R}^2 : \|w - u\| = d, |\langle \eta, w - u \rangle| > \|w - u\| \cos \delta\}.$$

Under the assumption that $B_\lambda(u, r) \approx B(u, r/\sqrt{\lambda(u)})$ and

$$\lambda(v) \approx \lambda(u), \quad \text{for all } v \in B_\lambda(u, r),$$

this edge correction ensures approximate unbiasedness in the isotropic case (29).

In order to find a powerful statistic for a test of locally rescaled against retransformed second-order stationarity, consider again transformation of a stationary point process along one direction η . The transformation has an opposite effect on the orientational K -functions with respect to the direction η and the orthogonal direction η^\perp ; therefore, we suggest to use the difference

$$\begin{aligned} \Delta K_{\text{dir}}(r; \eta, \delta) &= K_0(r; \eta, \delta) - K_0(r; \eta^\perp, \delta) \\ &= \int_{B(O, r)} g_0(u) (\mathbf{1}(|\langle \eta, u \rangle| > \|u\| \cos \delta) - \mathbf{1}(|\langle \eta, u \rangle| < \|u\| \sin \delta)) du. \end{aligned} \quad (36)$$

Redenbach et al. (2009) considered a closely related statistic for detecting anisotropy in 3D point processes and found it to be slightly more powerful than the distribution of nearest neighbour distances restricted to a subset of orientations. Obviously, it does not make sense to consider sectors with $\delta > \pi/4$ here. If $g_0(u) = g_0(\|u\|)$, $\Delta K_{\text{dir}}(r; \eta, \delta) = 0$, compare also with Figure 8.

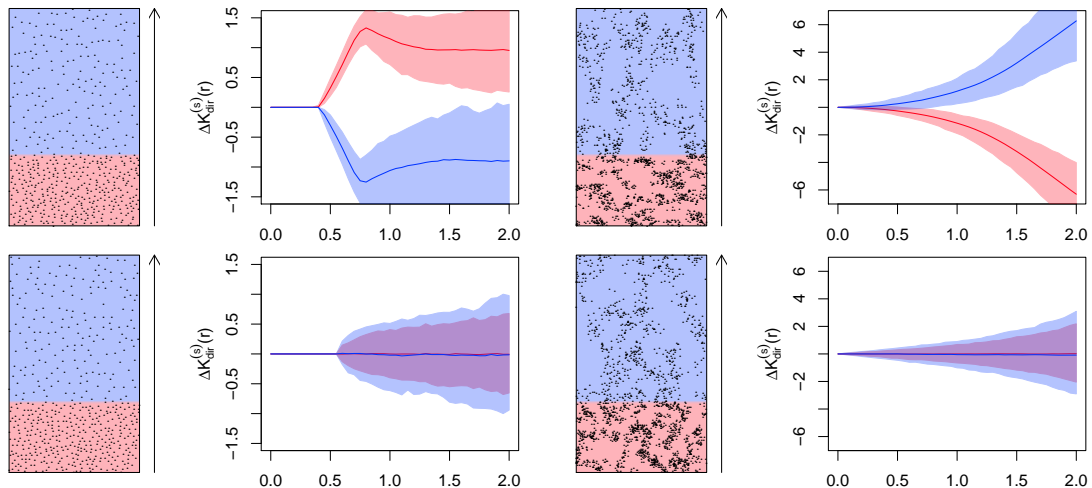


Figure 8: Realizations of retransformed (top row) and locally rescaled (bottom row) point processes, and corresponding ΔK_{dir} -functions. Arrows indicate the reference direction; sector width was set to $2\delta = \pi/2$. Plots of the ΔK_{dir} -functions estimated on the subwindows of high and low intensity (red and blue) show means and 90% pointwise envelopes based on 500 simulated realizations.

A test of locally rescaled second-order stationarity can now be constructed as described in the previous Section 5.1, by replacing estimates of K_0 with estimates of ΔK_{dir} . The reference direction η may be chosen arbitrarily, but for maximum power against the alternative of retransformed second-order stationarity, it is a good idea to let η represent the gradient direction of the transformation, which is directly linked to the gradient of the intensity function.

The hypothesis of retransformed second-order stationarity with respect to a known transformation h can be tested as described above, using the corresponding statistic $K_0(r; \eta, \delta)$. Estimates of this statistic are obtained from the back-transformed point pattern, which is a realization of a second-order stationary point process under the hypothesis. This approach is taken in the analysis of the bronze data in Section 6.1.

6 Data analysis

6.1 The bronze data

The bronze pattern represents centres of sphere profiles in a dense packing, with sphere diameter varying along one direction (identified as the x -direction in what follows). This gives rise to expect that the data are well described by a locally rescaled second-order stationary model. As a first step in the analysis of this point pattern, the intensity function, depicted in Figure 9, was estimated by kernel smoothing of the x -coordinate. We used the function `rho` from the R-library `spatstat` (Baddeley and Turner, 2006).

For the tests of locally rescaled second-order stationarity as described in Section 5, we first split the original window into two parts containing the same number

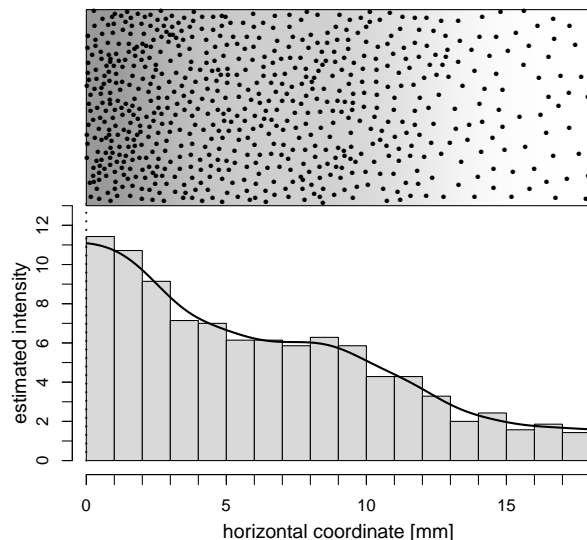


Figure 9: Intensity function used in the analysis of the bronze point pattern, size $18 \text{ mm} \times 7 \text{ mm}$. Top: point pattern with background shaded according to kernel density estimate of the intensity. Bottom: intensity estimated on parallel slices of 1 mm width, and kernel estimate.

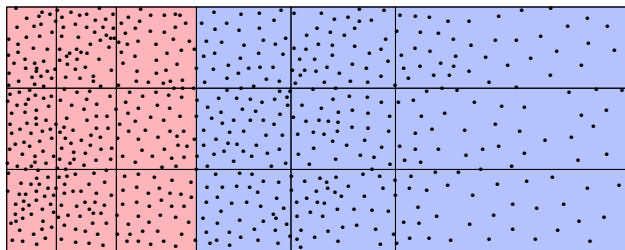


Figure 10: Partition of the bronze point pattern into two sets of 9 quadrats as used in the tests on reweighted and locally rescaled second-order stationarity.

of points. Each part was then subdivided into 9 quadrats, with number of points ranging from 34 to 42, see Figure 10.

For the test of locally rescaled second-order stationarity, $\widehat{K}_0^{(s)}$ was determined on the interval $[0, r_0]$ with $r_0 = 1.25$ on each quadrat. For the test on reweighted second-order stationarity, we used estimates $\widehat{K}_0^{(w)}$ on $[0, 0.4]$, which corresponds roughly to $r_0 = 1.25/\sqrt{\sup \lambda}$. The K -function estimates are shown in Figure 11. The locally rescaled K -functions are quite similar on the test set with high intensity (red) and with low intensity (blue). Accordingly, the results of the permutation test are non significant: with the test statistic T given in (32), the test yields a p -value of $p = 0.28$, and with the more robust statistic \bar{T} given in (33), we obtain $p = 0.34$. By contrast, the corresponding tests on reweighted second-order stationarity are highly significant, namely $p = 0.002$ when T is applied, and $p = 0.001$ when \bar{T} is used. In order to test retransformed second-order stationarity, an appropriate back-transformation h^{-1} has to be determined. When the intensity λ only depends on one coordinate, a very simple approach consists in rank-transforming that coordi-

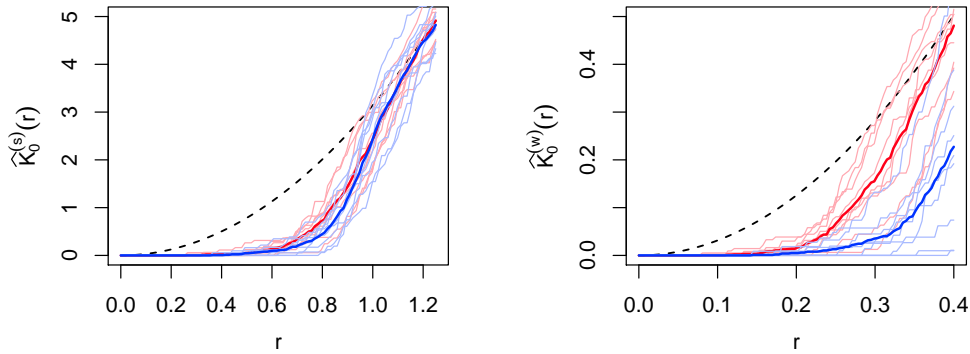


Figure 11: Estimates of the locally rescaled K -function (left) and of the reweighted K -function (right) obtained on the test quadrats, and mean K -functions (fat lines) for each of the test sets. The colours correspond to Figure 10; the dashed line represents the Poisson K -function, $K(r) = \pi r^2$.

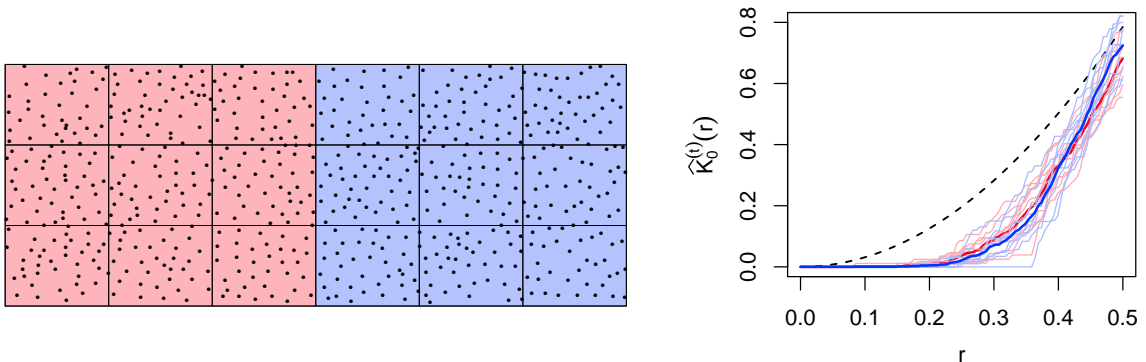


Figure 12: Left: The bronze pattern, transformed back to homogeneity on the original window, is split into two sets of quadrats containing approximately the same number of points. Right: Estimates $\hat{K}_0^{(t)}$ on the quadrats, and mean of $\hat{K}_0^{(t)}$ on the two test sets, with colours corresponding to the left figure.

nate. That approach is taken e.g. by Fleischer et al. (2006a,b). Since we anyway had estimated λ before, we estimated h^{-1} from the integral of the estimated intensity $\hat{\lambda}$ along the x -axis, mapping the observation window onto itself (Figure 12), see also Appendix A. Estimates of K_0 of the original pattern \mathbf{x} are then simply obtained by estimating the stationary K function on the backtransformed pattern $h^{-1}(\mathbf{x})$, cf. (26). The test results were non significant ($p = 0.33$ and $p = 0.35$), using $r_0 = 0.5$ as upper bound, which corresponds to $1.2/\sqrt{\bar{\lambda}}$, where $\bar{\lambda} = 5.4$ is the estimate for the stationary intensity from the backtransformed pattern. This result was expected, since the K -function cannot detect anisotropy. A plot of segments connecting nearest neighbours however reveals the distinct local anisotropy in the backtransformed pattern (Figure 13).

The test of retransformed second-order stationarity given in Section 5.2 underpins this finding, yielding highly significant results ($p = 0.001$ with test statistic T , and $p = 0.0005$ with \bar{T}). For this test, we estimated the difference ΔK_{dir} between orientational template K -functions, evaluated on bisectors of width $2\delta = \pi/2$ centred around the x - and y -direction. The resulting estimates of the ΔK_{dir} -functions are shown in Figure 14, left part. Carried out on the original pattern, the same type of test gave non significant results with $p > 0.89$ (Figure 14, right part).

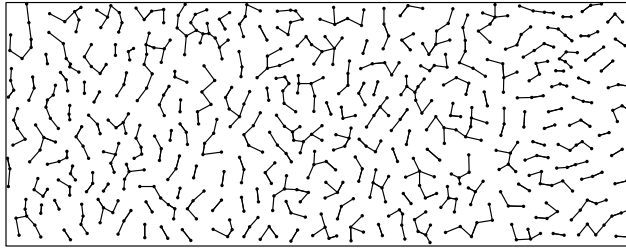


Figure 13: Pairs of nearest neighbours in the backtransformed bronze pattern. Apparently, the preferred nearest neighbour direction changes along the x -direction.

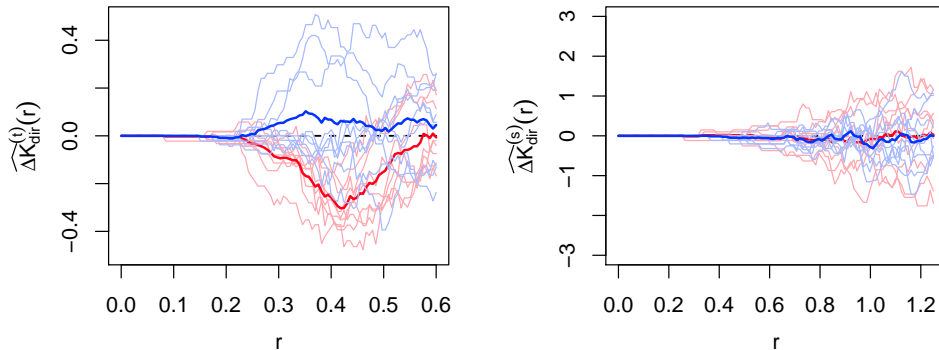


Figure 14: Difference of orthogonal orientational template K -functions, estimated on quadrats, and means over test sets, for the backtransformed pattern (left) and the original pattern (right).

6.2 The *Beilschmiedia* data

The *Beilschmiedia* pattern exhibits extreme differences in local plant density and strong clustering. It is believed that the density is heavily influenced by the terrain covariates altitude and norm of the altitude gradient. Therefore, Waagepetersen (2007) and Møller and Waagepetersen (2007) fit inhomogeneous cluster point processes to these data. They use a log-linear model for the intensity as a function of the covariates, and estimate the intensity by a Bayesian approach and maximum likelihood, respectively (Figure 15).

For the test of reweighted second-order stationarity, we partitioned the pattern into 4×8 quadrats. Only quadrats with more than 30 points were included in the test. In lack of a natural intensity gradient, we used the observed number of points to assign the remaining quadrats to two test sets (Figure 16).

The number of points in the quadrats used for the test varies hugely, from 32 to 404. Therefore, we only considered the more robust test statistic \bar{T} . The results are highly significant ($p = 0.001$ and $p = 0.0002$); the estimated template K -functions indicate strong clustering for most of the quadrats with many points, and repulsion on most of the quadrats with fewer points, see Figure 17.

This result does not necessarily imply that the *Beilschmiedia* pattern cannot be described by a reweighted second-order stationary point process, but could also be due to an inappropriate intensity estimate. We therefore also investigated a nonparametric intensity estimate. Kernel estimators with constant bandwidth seem to be ruled out by the strongly varying intensity. We applied an adaptive estimate

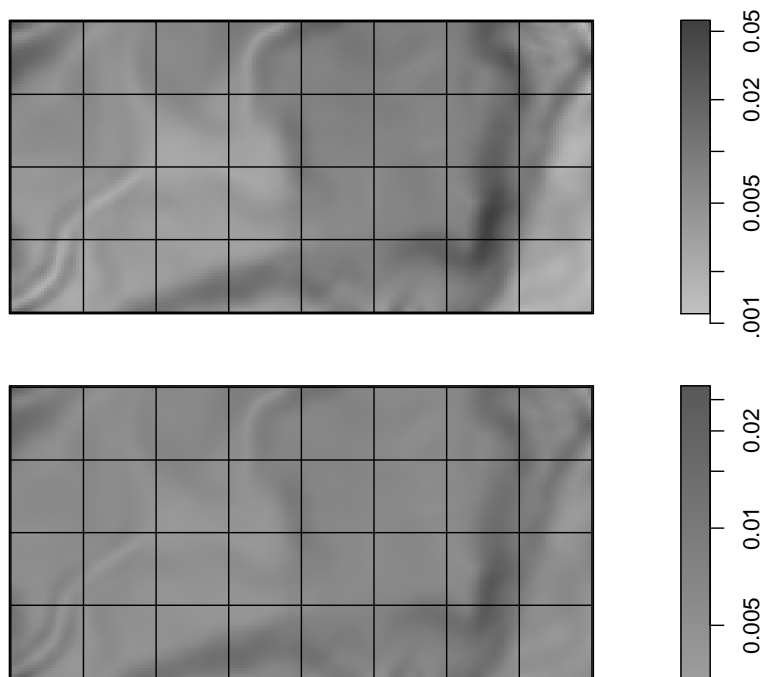


Figure 15: Bayesian (top) and maximum likelihood (bottom) intensity estimate for the *Beilschmiedia* data set, as in Møller and Waagepetersen (2007). The plot is subdivided into 8×4 quadrats.

available in the R-library `spatstat` as function `adaptive.density`. This estimator was originally suggested by Ogata et al. (2003), and is based on Voronoi tessellations of randomly thinned patterns. The intensity estimate used in the test is shown in Figure 18. The corresponding test result was non significant ($p = 0.16$).

In order to make the estimate more robust in cases of strong inhomogeneity, an optional renormalisation of $\hat{K}^{(w)}$ is implemented in the R package `spatstat`. With the recommended parameter `normpower=2`, it amounts to rescaling the estimated intensity function $\hat{\lambda}$ on the evaluation window or quadrat B by a factor $c(\hat{\lambda}, \mathbf{X}_B) = \sum_{u \in \mathbf{X}_B} 1/(|B|\hat{\lambda}(u))$. If $\hat{\lambda}$ is proportional to λ , the mean value of the correction factor becomes $\mathbb{E}c(\hat{\lambda}, \mathbf{X}_B) = \lambda(\cdot)/\hat{\lambda}(\cdot)$, which follows by application of Campbell’s formula. Therefore, renormalisation can also improve $\hat{K}^{(w)}$ in the case of systematic proportional error of $\hat{\lambda}$. With renormalised estimates of K_0 , the test yielded non significant p -values $p > 0.85$ in all three cases.

6.3 The *Scholtzia* data

At the first glance, the *Scholtzia* pattern may appear as a realization of a locally scaled point process — the point patterns on the quadrats in Figure 19 (right part) could be taken to represent scaled versions of the same template process. With only 171 points, the data set is almost too small for a statistical analysis that requires subdivision. Nevertheless, we applied the tests of locally rescaled and reweighted second-order stationarity to the point pattern, based on only four quadrats in each test set, and using the test statistic \bar{T} . A kernel estimate $\hat{\lambda}$ was used for the intensity

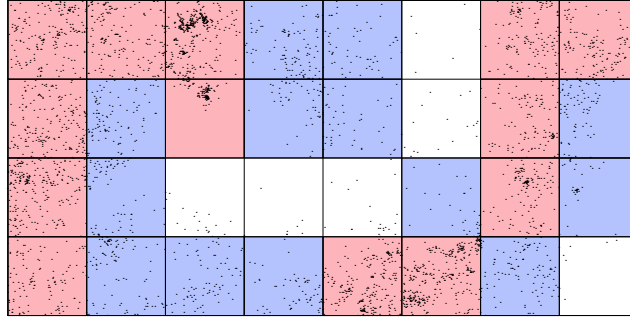


Figure 16: Two test sets of quadrats that were used in the analysis of the *Beilschmiedia* data set.

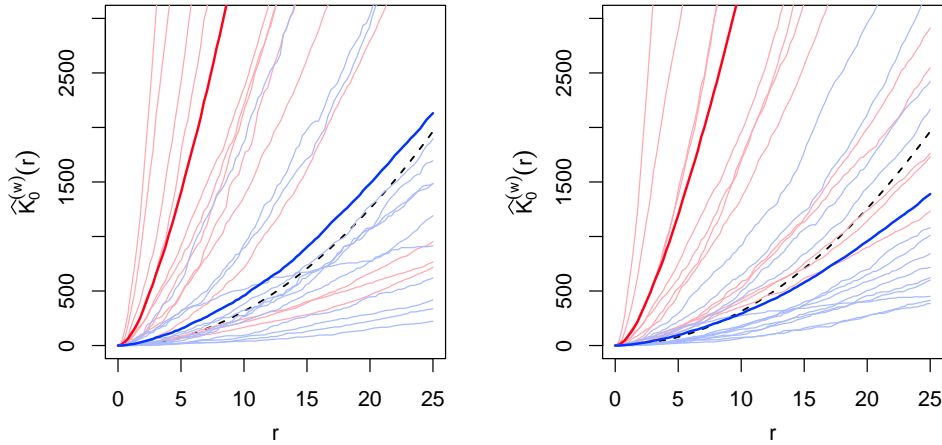


Figure 17: $\hat{K}_0^{(w)}$ using Bayesian (left) and maximum likelihood (right) intensity estimate, evaluated on the test quadrats. Colours correspond to Figure 16, fat lines: mean over the test sets. Dashed line: K -function for a Poisson point process.

function (left part of Figure 19), namely the estimator provided by the function density from the R-library `spatstat`, with default parameters. With the division into quadrats, we tried to follow the estimated intensity while sticking to simple geometrical shapes.

When using the original $\hat{\lambda}$ estimates in the calculation of the estimates $\hat{K}_0^{(s)}$ and $\hat{K}_0^{(w)}$, the tests yielded significant results with $p = 0.03$. Both $\hat{K}_0^{(s)}$ and $\hat{K}_0^{(w)}$ lie above the Poisson- K -function $K(r) = \pi r^2$, when estimated on the quadrats with high intensity (marked red in Figure 20), and below πr^2 for the quadrats with low intensity (blue). This is possibly due to a bias of $\hat{\lambda}$ as is typical for kernel estimators, resulting in overestimation of $\hat{\lambda}$ in regions where λ is low, and underestimation of high λ . Since $\hat{\lambda}$ appears in the denominator of \hat{K} , the K -function tends to be underestimated in regions of low intensity and vice versa. After renormalisation, the difference between the two subsets became non significant, with $p = 0.29$ and $p = 0.26$, respectively, for the tests of locally rescaled or reweighted second-order stationarity, see Figure 20. The estimates are now very close to the Poisson- K -function.

Although the initial significance turned into non significance by using a more robust estimator for the K -functions, one might still question the hypothesis that

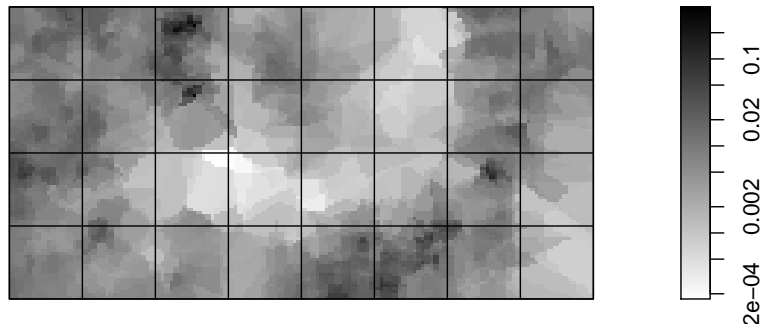


Figure 18: Nonparametric intensity estimate for the *Beilschmiedia* data, as used in the present paper.

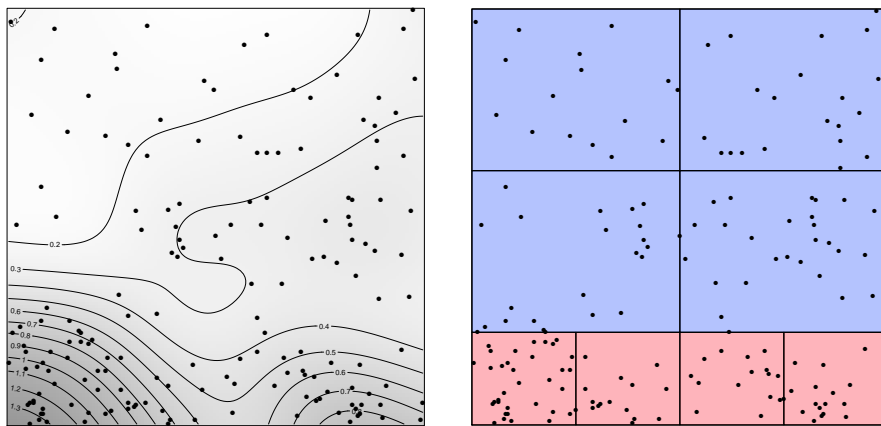


Figure 19: Left: nonparametric estimate for the intensity function of the *Scholtzia* as used in the model tests, right: partition into quadrats for the tests on reweighted and locally rescaled second-order stationarity.

the *Scholtzia* pattern is hidden second-order stationary. This case shows that one should be cautious when assigning an observed inhomogeneous point pattern to one of the models just based on its visual appearance. While working on the paper Prokešová et al. (2006), the authors were convinced that the *Scholtzia* pattern is well described by a locally rescaled second-order stationary model.

7 Discussion

For the bronze and *Scholtzia* point patterns analyzed in the data section, the division of the point pattern into quadrats with roughly the same number of points was done in an ad hoc manner. In the more difficult case of the *Beilschmiedia* pattern where the inhomogeneity is pronounced and does not follow a given direction, it is more challenging to find an appropriate subdivision of the pattern. We took a pragmatic approach and partitioned the observation window into quadrats of equal area, excluding quadrats with too few points. An alternative is automatic partitioning, using a Voronoi tessellation based on an inhomogeneous point process with intensity λ_g proportional to the intensity λ of the point process in question, that is, λ_g

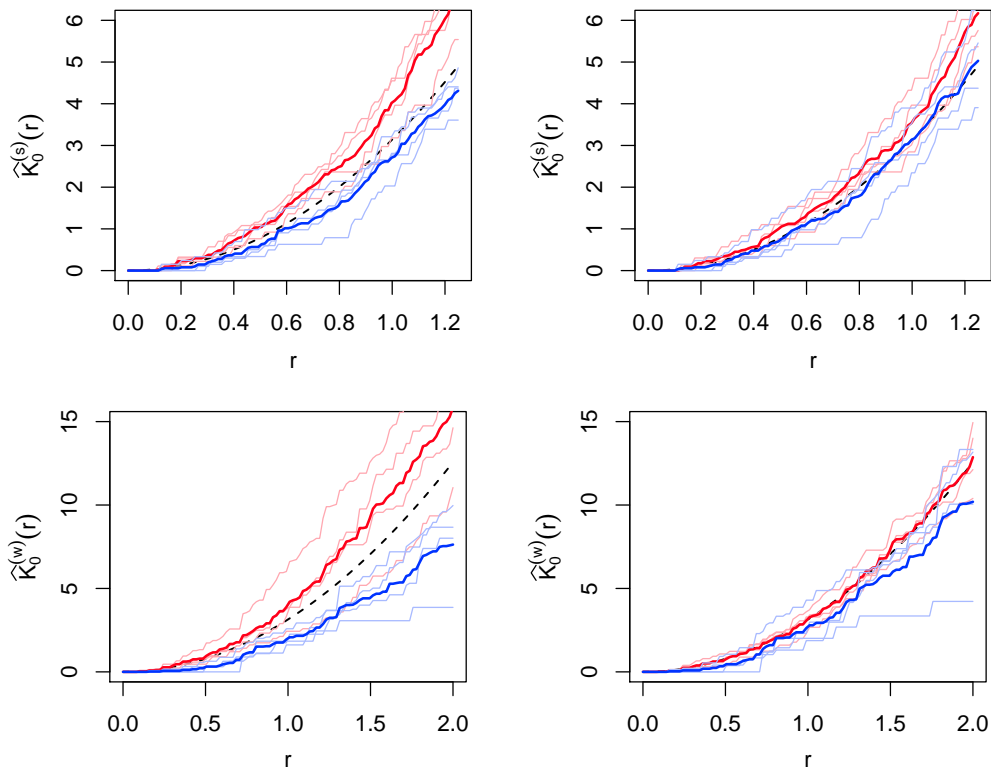


Figure 20: Estimates for the template K -function of the *Scholtzia* pattern, assuming different models for the inhomogeneity, obtained on the high intensity subplot (red) and the low intensity subplot (blue) as shown in Figure 19. The dashed line stands for the Poisson- K -function. Top: locally rescaled template K -function, bottom: reweighted. Left: using $\hat{\lambda}$ as is, right: with renormalised intensity estimate $\hat{\lambda}$.

is chosen such that $\lambda(u)/\lambda_g(u) = c$ for all points u in the observation window. Locally scaled repulsive Strauss processes as described in Hahn et al. (2003) or locally scaled Matérn hard core point processes would constitute natural candidates, since Voronoi tessellations with respect to such point processes consist of cells of roughly the same size in the stationary case. Voronoi cells with respect to a stationary germ point process have mean area that is inversely proportional to the intensity of the germ point process. This inverse proportionality approximately carries over if the germ points form a locally scaled inhomogeneous point process, given the intensity is fairly slowly varying. If λ can be considered roughly constant in the vicinity of an arbitrary germ point u , the Voronoi cell $V(u)$ belonging to u would contain an expected number $\lambda(u)|V(u)| \approx \lambda(u)/\lambda_g(u) = c$ of points.

For each of the three types of hidden second-order stationarity considered in the present paper, the estimate of the template K -function depends on the intensity function of the inhomogeneous process or the transformation involved. As emphasized by the results in the data section, the resulting inference is very sensitive to the quality of the estimate of the intensity function. The bronze data went smoothest, because it is regular and the estimate of the intensity function has a small variance. For the Beilschmiedia data, a parametric model for the intensity function based on auxiliary variables about the terrain topology (Waagepetersen, 2007; Møller and

Waagepetersen, 2007) did not provide a fully satisfactory intensity estimate which may be seen from direct simulations of the fitted model. A nonparametric intensity estimate was more appropriate. The hypothesis of reweighted second-order stationarity was rejected, when using the parametric intensity estimate, while accepted when using the nonparametric estimate. Two-step estimation procedures (Waagepetersen and Guan, 2009) are also very sensitive to the quality of the intensity function estimate. The same phenomenon is known from the stationary case.

A renormalisation procedure may improve the quality of the intensity function estimate, as discussed in the last paragraph of Section 6.2. An interesting future research topic would be a systematic study of such renormalisation procedures.

Acknowledgements

This research has been supported by Centre for Stochastic Geometry and Advanced Bioimaging, funded by a grant from the Villum Foundation.

A Constructions of transformations

If the intensity function of the resulting inhomogeneous process only depends on one coordinate or on the distance to a reference point, then there is a transformation with the same property that is differentiable (up to a set of Lebesgue measure zero) and one-to-one on a rectangular respectively circular sampling window.

To see this, let us first suppose that the intensity function depends on one coordinate only, $\lambda(x, y) = s(x)$, say. It is then natural to focus on transformations h of the form $h(x, y) = (t(x), y)$. Then, the requirement $Jh^{-1} \propto \lambda$ is equivalent to

$$(t^{-1})'(x) \propto s(x),$$

or

$$t^{-1}(x) = b \int_{x_0}^x s(v) dv + c,$$

for some real constants x_0 , b and c . The transformation h is determined by the additional requirement of being one-to-one on a rectangular sampling window $[x_0, x_1] \times [y_0, y_1]$ in which case

$$b = (x_1 - x_0) \left[\int_{x_0}^{x_1} s(v) dv \right]^{-1}, \quad c = x_0.$$

For instance, if

$$\lambda(x, y) = \begin{cases} \lambda_1 & \text{if } x < a \\ \lambda_2 & \text{if } x \geq a, \end{cases}$$

where $x_0 \leq a \leq x_1$, then

$$t^{-1}(x) = \begin{cases} b\lambda_1(x - x_0) + x_0 & \text{if } x < a, \\ b\lambda_1(a - x_0) + b\lambda_2(x - a) + x_0 & \text{if } x \geq a, \end{cases}$$

where

$$b = \frac{x_1 - x_0}{\lambda_1(a - x_0) + \lambda_2(x_1 - a)}.$$

As another important example, let us suppose that the intensity only depends on the distance to the origin, $\lambda(x, y) = s(\sqrt{x^2 + y^2})$, say. Here, it is natural to seek a solution among transformations h of the form

$$h(x, y) = t\left(\sqrt{x^2 + y^2}\right) \frac{(x, y)}{\sqrt{x^2 + y^2}}.$$

These transformations only change the distance to the origin. The transformation t then satisfies the following equation

$$t^{-1}(r) \cdot (t^{-1})'(r) \propto r \cdot s(r).$$

This equation can be used to express t in terms of s . We find

$$\begin{aligned} \int_0^r v \cdot s(v) dv &\propto \int_0^r t^{-1}(v)(t^{-1})'(v) dv \\ &= \int_{t^{-1}(0)}^{t^{-1}(r)} u du \\ &= \frac{t^{-1}(r)^2 - t^{-1}(0)^2}{2}. \end{aligned}$$

It follows that

$$t^{-1}(r) = \left[b \int_0^r v s(v) dv + c \right]^{1/2}$$

for some real constants b and c . The transformation is fully specified, if we require that h is one-to-one on a circular sampling window $B(O, R)$, then

$$b = R^2 \left[\int_0^R v s(v) dv \right]^{-1}, \quad c = 0.$$

For instance, if

$$s(r) = \lambda_0 \exp(-\beta r),$$

then

$$t^{-1}(r) = R \left[\frac{1 - e^{-\beta r}(\beta r + 1)}{1 - e^{-\beta R}(\beta R + 1)} \right]^{1/2}, \quad r \geq 0.$$

In the more general case where $\lambda(x, y) = s(\sqrt{x^2 + (\gamma \cdot y)^2})$, $\gamma > 0$, we can rescale the transformation obtained for $\gamma = 1$. If this transformation is called h_1 , then the transformation for general γ is obtained as follows

$$h_\gamma(x, y) = \frac{1}{\sqrt{\gamma}} h_1(x, \gamma \cdot y).$$

B Locally scaled Neyman-Scott processes

The locally scaled Neyman-Scott process has intensity function

$$\lambda(u) = \alpha \int_{\mathbb{R}^2} \alpha^{-1} c(x)^{-2} \cdot c(x)^{-2} k(c(x)^{-1} \|u - x\|) dx \approx c(u)^{-2}$$

and second-order product density

$$\begin{aligned} \lambda^{(2)}(u, v) &= \alpha^2 \int_{\mathbb{R}^2} \alpha^{-1} c(x)^{-2} \cdot c(x)^{-4} k(c(x)^{-1} \|u - x\|) k(c(x)^{-1} \|v - x\|) dx + \lambda(u)\lambda(v) \\ &\approx \alpha c(u)^{-2} c(v)^{-2} \int_{\mathbb{R}^2} k(\|y\|) k(\|y + \frac{u - v}{c_{u,v}}\|) dy + \lambda(u)\lambda(v), \end{aligned}$$

where $c_{u,v} = (c(u) + c(v))/2$, say. It follows that the pair correlation function of the locally scaled Neyman-Scott process satisfies

$$\begin{aligned} g(u, v) &\approx \alpha \int_{\mathbb{R}^2} k(\|y\|) k(\|y + \frac{u - v}{c_{u,v}}\|) dy + 1 \\ &= g_0\left(\frac{\|u - v\|}{c_{u,v}}\right), \end{aligned}$$

where g_0 is the pair correlation function of \mathbf{X}_0 , and (29) is approximately satisfied.

References

- Anselin, L. (1989). What is special about spatial data? Alternative perspectives on spatial data analysis. In *Spring 1989 Symposium on Spatial Statistics, Past, Present and Future, Department of Geography, Syracuse University*.
- Anselin, L. (1995). Local indicators of spatial association — LISA. *Geographical Analysis* 27(2), 93–115.
- Armstrong, P. (1991). Species patterning in heath vegetation of the northern sandplain. Honours thesis, Murdoch University, Western Australia.
- Baddeley, A. and R. Turner (2006). Modelling spatial point patterns in R. In A. Baddeley, P. Gregori, J. Mateu, R. Stoica, and D. Stoyan (Eds.), *Case Studies in Spatial Point Pattern Modelling*, Volume 185 of *Lecture Notes in Statistics*, pp. 23–74. New York: Springer-Verlag. ISBN: 0-387-28311-0.
- Baddeley, A. J., J. Møller, and R. Waagepetersen (2000). Non- and semi-parametric estimation of interaction in inhomogeneous point patterns. *Statistica Neerlandica* 54(3), 329–350.
- Bernhardt, R., F. Meyer-Olbersleben, and B. Kieback (1997). Fundamental investigation on the preparation of gradient structures by sedimentation of different powder fractions under gravity. In D. Hui (Ed.), *Proc. of the 4th Int. Conf. on Composite Engineering, July 6-12 1997, ICCE/4, Hawaii*, pp. 147–148.

- Condit, R. (1998). *Tropical Forest Census Plots*. Berlin, Germany and Georgetown, Texas: Springer-Verlag and R. G. Landes Company.
- Condit, R., S. P. Hubbell, and R. B. Foster (1996). Changes in tree species abundance in a neotropical forest: impact of climate change. *Journal of Tropical Ecology* 12, 231–256.
- Cox, D. R. (1955). Some statistical methods connected with series of events. *Journal of the Royal Statistical Society, Series B (Methodological)* 17(2), 129–164.
- Cressie, N. and L. B. Collins (2001a). Analysis of spatial point patterns using bundles of product density LISA functions. *Journal of Agricultural, Biological, and Environmental Statistics* 6(1), 118–135.
- Cressie, N. and L. B. Collins (2001b). Patterns in spatial point locations: Local indicators of spatial association in a minefield with clutter. *Naval Research Logistics* 48, 333–347.
- Diggle, P. J., N. Lange, and F. M. Benes (1991). Analysis of variance for replicated spatial point patterns in clinical neuroanatomy. *Journal of the American Statistical Association* 86(415), 618–625.
- Diggle, P. J., J. Mateu, and H. E. Clough (2000). A comparison between parametric and non-parametric approaches to the analysis of replicated spatial point patterns. *Advances in Applied Probability* 32(2), 331–343.
- Fleischer, F., M. Beil, M. Kazda, and V. Schmidt (2006a). Analysis of spatial point patterns in microscopic and macroscopic biological image data. In A. Baddeley, P. Gregori, J. Mateu, R. Stoica, and D. Stoyan (Eds.), *Case studies in spatial point processes models*, Number 185 in Lecture Notes in Statistics, pp. 235–260. New York: Springer.
- Fleischer, F., S. Eckel, I. Schmidt, V. Schmidt, and M. Kazda (2006b). Point process modelling of root distribution in pure stands of *Fagus sylvatica* and *Picea abies*. *Canadian Journal of Forest Research* 36, 227–237.
- Fry, N. (1979). Random point distributions and strain measurement in rocks. *Tectonophysics* 60(1), 89–105.
- Getis, A. and J. Franklin (1987). Second-order neighborhood analysis of mapped point patterns. *Ecology* 68(3), 473–477.
- Guan, Y. (2008a). On consistent nonparametric intensity estimation for inhomogeneous spatial point processes. *Journal of the American Statistical Association* 104, 1238–1247.
- Guan, Y. (2008b). Variance estimation for statistics computed from inhomogeneous spatial point processes. *Journal of the Royal Statistical Society, Series B* 70(1), 175–190.

- Guan, Y. (2009a). Fast block variance estimation procedures for inhomogeneous spatial point processes. *Biometrika* 96(1), 213–220.
- Guan, Y. (2009b). On nonparametric variance estimation for second-order statistics of inhomogeneous spatial point processes with a known parametric intensity form. *Journal of the American Statistical Association* 104(488), 1482–1491.
- Guan, Y. and J. M. Loh (2007). A thinned block bootstrap variance estimation procedure for inhomogeneous spatial point patterns. *Journal of the American Statistical Association* 102(480), 1377–1386.
- Guan, Y. and Y. Shen (2010). A weighted estimating equation approach for inhomogeneous spatial point processes. *Biometrika* 97(4), 867–880.
- Hahn, U. (2007). *Global and Local Scaling in the Statistics of Spatial Point Processes*. Habilitationsschrift, Universität Augsburg.
- Hahn, U. (2012). A studentized permutation test for the comparison of spatial point patterns. *Journal of the American Statistical Association* 107(498), 754–764.
- Hahn, U., E. B. V. Jensen, M. N. M. van Lieshout, and L. S. Nielsen (2003). Inhomogeneous spatial point processes by location-dependent scaling. *Advances in Applied Probability* 35, 319–336.
- Hahn, U., A. Micheletti, R. Pohlink, D. Stoyan, and H. Wendrock (1999). Stereological analysis and modelling of gradient structures. *Journal of Microscopy* 195(2), 113–124.
- Hellmund, G., M. Prokešová, and E. B. V. Jensen (2008). Lévy based Cox point processes. *Advances in Applied Probability* 40(3), 603–629.
- Ho, L. P. and S. N. Chiu (2006). Testing the complete spatial randomness by Diggle’s test without an arbitrary upper limit. *Journal of Statistical Computation and Simulation* 76(7), 585–591.
- Hubbel, S. P. and R. B. Foster (1983). Diversity of canopy trees in a neotropical forest and implications for conservation. In S. L. Sutton, T. C. Whitmore, and A. C. Chadwick (Eds.), *Tropical Rain Forest: Ecology and Management*, pp. 25–41. Blackwell Scientific Publications.
- Illian, J., A. Penttinen, H. Stoyan, and D. Stoyan (2008). *Statistical analysis and modelling of spatial point patterns*. Statistics in Practice. Chichester: John Wiley & Sons Ltd.
- Jensen, E. B. V. and L. S. Nielsen (2000). Inhomogeneous Markov point processes by transformation. *Bernoulli* 6, 721–782.
- Jensen, E. B. V. and L. S. Nielsen (2001). A review on inhomogeneous spatial point processes. In I. V. Basawa, C. C. Heyde, and R. L. Taylor (Eds.), *Selected Proc. Symp. Inference for Stoch. Processes*, Number 37 in IMS Lecture Notes Monogr. Ser. Beachwood, OH, pp. 297–318. Institute of Mathematical Statistics.

- Matérn, B. (1960). Spatial variation. *Meddelanden från Statens skogsforskningsinstitut* 49(5), 1–144. Second edition: Matérn (1986).
- Møller, J. and R. P. Waagepetersen (2003). *Statistical Inference and Simulation for Spatial Point Processes*. Boca Raton, Florida: Chapman & Hall / CRC.
- Møller, J. and R. P. Waagepetersen (2007). Modern statistics for spatial point processes. *Scandinavian Journal of Statistics* 34, 643–684.
- Neyman, J. and E. L. Scott (1958). Statistical approach to problems of cosmology. *Journal of the Royal Statistical Society, Series B (Methodological)* 20(1), 1–43.
- Nielsen, L. S. and E. B. V. Jensen (2004). Statistical inference for transformation inhomogeneous point processes. *Scandinavian Journal of Statistics* 31(1), 131–142.
- Ogata, Y., K. Katsura, and M. Tanemura (2003). Modelling heterogeneous space–time occurrences of earthquakes and its residual analysis. *Journal of the Royal Statistical Society: Series C (Applied Statistics)* 52(4), 499–509.
- Ohser, J. and D. Stoyan (1981). On the second-order and orientation analysis of planar stationary point processes. *Biometrical Journal* 23(6), 523–533.
- Prokešová, M. (2010). Inhomogeneity in spatial Cox point processes — location dependent thinning is not the only option. *Image Analysis & Stereology* 29(3), 133–141.
- Prokešová, M., U. Hahn, and E. B. V. Jensen (2006). Statistics for locally scaled point patterns. In A. Baddeley, P. Gregori, J. Mateu, R. Stoica, and D. Stoyan (Eds.), *Case Studies in Spatial Point Pattern Modelling*, Number 185 in Lecture Notes in Statistics, pp. 99–123. New York: Springer-Verlag.
- Redenbach, C., A. Särkkä, J. Freitag, and K. Schladitz (2009). Anisotropy analysis of pressed point processes. *AStA Advances in Statistical Analysis* 93(3), 237–261.
- Ripley, B. D. (1976). The second-order analysis of stationary point processes. *Journal of Applied Probability* 13, 255–266.
- Ripley, B. D. (1979). Tests of 'randomness' for spatial point patterns. *Journal of the Royal Statistical Society, Series B (Methodological)* 41(3), 368–374.
- Shimatani, K. and Y. Kubota (2004). Spatial analysis for continuously changing point patterns along a gradient and its application to an abies sachalinensis population. *Ecological Modelling* 180, 359–369.
- Stoyan, D. and V. Beneš (1991). Anisotropy analysis for particle systems. *Journal of Microscopy* 164(2), 159–168.
- Thomas, M. (1949). A generalization of Poisson's binomial limit for use in ecology. *Biometrika* 36(1/2), 18–25.

- van Lieshout, M. N. M. (2011). A J -function for inhomogeneous point processes. *Statistica Neerlandica* 65(2), 183–201.
- Waagepetersen, R. P. (2007). An estimating function approach to inference for inhomogeneous Neyman-Scott processes. *Biometrics* 63, 252–258.
- Waagepetersen, R. P. and Y. Guan (2009). Two-step estimation for inhomogeneous spatial point processes, simulation study. *Journal of the Royal Statistical Society, Series B* 71(3), 685–702.